




Article

Effects of Particle Size on the Dielectric, Mechanical, and Thermal Properties of Recycled Borosilicate Glass-Filled PTFE Microwave Substrates

Ibrahim Abubakar Alhaji ^{1,2}, Zulkifly Abbas ^{1,3,*}, Mohd Hafiz Mohd Zaid ^{1,4} and Ahmad Mamoun Khamis ¹

- ¹ Department of Physics, Faculty of Science, Universiti Putra Malaysia, Serdang 43400, Malaysia; gs54099@student.upm.edu.my (I.A.A.); mhmzaid@upm.edu.my (M.H.M.Z.); akhameis@yahoo.com (A.M.K.)
- ² Department of Physics, Faculty of Science, Federal University of Kashere, Gombe PMB 0182, Gombe State, Nigeria
- ³ Institute of Tropical Forestry and Forest Product, Universiti Putra Malaysia, Serdang 43400, Malaysia
- ⁴ Institute of Advanced Technology, Universiti Putra Malaysia, Serdang 43400, Malaysia
- * Correspondence: za@upm.edu.my; Tel.: +60-17-330-0429

Abstract: Low dielectric loss and low-cost recycled borosilicate (BRS) glass-reinforced polytetrafluoroethylene (PTFE) composites were fabricated for microwave substrate applications. The composites were prepared through a dry powder processing technique by dispersing different micron sizes (25 μm , 45 μm , 63 μm , 90 μm , and 106 μm) of the recycled BRS filler in the PTFE matrix. The effect of the filler sizes on the composites' thermal, mechanical, and dielectric properties was studied. The dielectric properties of the composites were characterised in the frequency range of 1–12 GHz using an open-ended coaxial probe (OCP) connected to a vector network analyser (VNA). XRD patterns confirmed the phase formation of PTFE and recycled BRS glass. The scanning electron microscope also showed good filler dispersion at larger filler particle sizes. In addition, the composites' coefficient of thermal expansion and tensile strength decreased from 12.93 MPa and 64.86 ppm/ $^{\circ}\text{C}$ to 7.12 MPa and 55.77 ppm/ $^{\circ}\text{C}$ when the filler size is reduced from 106 μm to 25 μm . However, moisture absorption and density of the composites increased from 0.01% and 2.17 g/cm³ to 0.04% and 2.21 g/cm³. The decrement in filler size from 106 μm to 25 μm also increased the mean dielectric constant and loss tangent of the composites from 2.07 and 0.0010 to 2.18 and 0.0011, respectively, while it reduced the mean signal transmission speed from 2.088×10^8 m/s to 2.031×10^8 m/s. The presented results showed that PTFE/recycled BRS composite exhibited comparable characteristics with commercial high-frequency laminates.

Keywords: recycled borosilicate; PTFE; sintering; permittivity; high-frequency; substrates



Citation: Alhaji, I.A.; Abbas, Z.; Mohd Zaid, M.H.; Khamis, A.M. Effects of Particle Size on the Dielectric, Mechanical, and Thermal Properties of Recycled Borosilicate Glass-Filled PTFE Microwave Substrates. *Polymers* **2021**, *13*, 2449. <https://doi.org/10.3390/polym13152449>

Academic Editor: Alexey V. Lyulin

Received: 18 June 2021

Accepted: 19 July 2021

Published: 26 July 2021

Publisher's Note: MDPI stays neutral with regard to jurisdictional claims in published maps and institutional affiliations.



Copyright: © 2021 by the authors. Licensee MDPI, Basel, Switzerland. This article is an open access article distributed under the terms and conditions of the Creative Commons Attribution (CC BY) license (<https://creativecommons.org/licenses/by/4.0/>).

1. Introduction

The last decade has seen rapid and unprecedented developments in information technology driven by military and consumer markets [1–3]. This change creates demands for high-speed, light and low-cost microwave substrate. A microwave substrate that meets specific criteria supports microwave circuits [4–6]. Microwave substrates are dielectric materials with low permittivity and a low loss tangent at microwave frequencies [5]. The substrate materials should have the following properties: low permittivity and loss tangent for rapid signal propagation, low coefficient of thermal expansion (CTE) for dimensional stability, high thermal conductivity for transporting the heat generated away from the microwave circuit and good mechanical strength for material rigidity [7].

Polymers are employed for substrate applications due to their excellent electrical properties. Polytetrafluoroethylene (PTFE) is the most widely used among polymers because of its low permittivity, dielectric loss, moisture absorption and chemical inertness [8–10]. However, it has a high CTE (~109 ppm/ $^{\circ}\text{C}$) and melting point (~327 $^{\circ}\text{C}$) that hinder its utilisation [11]. It also lacks rigidity for practical substrate applications. These limitations

can be overcome by adding inorganic and rigid fillers such as glass with lower CTE and moderate dielectric properties. That is possible because the properties of polymers depend on their microstructure and composition [12]. The high melting point of PTFE can also be circumvented by employing a processing technique, such as the powder processing method, that does not require heat treatment to mix PTFE-glass composites [13].

Recently, recycled glass fillers have attracted considerable attention for microwave applications due to their rigidity and moderate dielectric properties [14]. Recycled glass is cheaper and reduces environmental pollution. In this work, the preparation and characterisation of recycled borosilicate glass filled PTFE substrate is reported. Borosilicate (BRS) is an industrial glass with a thermal conductivity ranging from 1–1.3 W/mK. It has a low CTE of 3.2 ppm/°C–4.0 ppm/°C and tensile strength of about 22 MPa–32 MPa. The glass is also an excellent electrical insulator with a dielectric constant and loss factor of 4.65–6.00 and 0.01–0.017 [15,16]. These excellent properties of BRS glass make it a perfect filler when recycled for PTFE-based substrate applications. To the best of our knowledge, no systematic study of the effect of the recycled BRS filler size on PTFE/recycled BRS composites has been reported. Therefore, this work investigated the dielectric, thermal, and mechanical properties of PTFE/recycled BRS. In addition, signal propagation speed across the composites with different filler sizes was calculated and analysed. The PTFE/recycled BRS composite was also compared with commercial high-frequency laminates.

2. Materials and Methods

2.1. Materials

The PTFE of type MF90C with an average particle size of 50–110 μm was obtained from Fujian Sannong New Materials Co., Ltd., Sanming, China. At the same time, BRS glass was acquired from Top Globe Sdn. Bhd. Selangor, Malaysia, in the form of waste moulds.

Glass Powder Preparation

The BRS glass moulds were initially cleaned, washed, and dried at room temperature for 24 h. After that, the moulds were crushed with a hammer into glass pebbles. A Plunger was further used to grind the glass pebbles into coarse glass powder. In addition, the coarse glass powder was transferred to a grinding mill jar with a powder-to-ball ratio of 20:1, which was then milled. The milling was conducted at room temperature for 24 h at 45 rpm using the U.S. Stoneware Jar Mills (U.S. Stoneware, East Palestine, OH, USA). After the milling stage, the recycled BRS powder was sieved to 25 μm , 45 μm , 63 μm , 90 μm , and 106 μm particle sizes. The range of these representative filler particle sizes is given in Table 1.

Table 1. Particle size distribution.

Representative Particle Size (μm)	Range of Particle Size (μm)
25	$X_1 \leq 25$
45	$25 < X_2 \leq 45$
63	$45 < X_2 \leq 63$
90	$63 < X_2 \leq 90$
106	$90 < X_2 \leq 106$

2.2. Preparation of PTFE/Recycled BRS Composites

The PTFE/recycled BRS composites were prepared by mixing 25 μm , 45 μm , 63 μm , 90 μm , and 106 μm of the recycled BRS filler with PTFE through a dry powder processing technique. The mixing was conducted via a Wing dry mixer for 10 min, and filler content in each composite was fixed at 5 wt.%. Then, the compositions were pressed into preforms using a hydraulic press at a pressure of 10 MPa for 5 min. The compacted composites were mechanically weak due to air voids. Hence, sintering is required for the removal of the voids. The samples were sintered from room temperature to 380 °C with a temperature rising time of 3 °C/min and held for 1 h to allow for particles fusion, coalescence and void elimination in the composites. The cooling rate was set at 1 °C/min from 380 °C to room

temperature to complete the sintering cycle. A Drying Oven (Jiangsu Sunkoo Machine Tech Co., Ltd., Changzhou, China) was utilised for the sintering.

2.3. Characterisations

2.3.1. Phase, Morphology and Composition

In this work, XRD was employed to analyse the phase formation of recycled BRS powder and PTFE/recycled BRS composites. The XRD data were collected using an automated Philips X'pert system (Model PW3040/60 MPD) with Cu-K α radiation operating at a voltage of 40.0 kV and a current of 40.0 mA with a wavelength of 1.5405 Å. The 2-theta range of 10°–70° with a scanning speed of 2.0 °/min was used to record the diffraction patterns. All data were exposed to the Rietveld analysis on X'Pert Highscore Plus v3.0 software (PANalytical B.V., Almelo, The Netherlands). The samples were classified by comparing their diffraction peaks with the Inorganic Crystal Structure Database (ICSD).

The shape, arrangement and dispersion of the recycled BRS particles in the composites were investigated using LEO 1455 Variable Pressure Scanning Electron Microscope (VPSEM, Leo Electron Microscopy Group, Oberkochen, Germany). The elemental composition of the samples was obtained via an Oxford Inca energy dispersive X-ray micro-analyser (EDX, Oxford Instruments, Buckinghamshire, England) attached to the Leo 1455 VPSEM. Five spots on each sample were examined with the EDX for accurate determination of the elemental compositions of the composites qualitatively.

2.3.2. Moisture Absorption

The presence of moisture within a material increases its dielectric properties [17]. This change degrades the performance of the materials. Thus, determining the moisture absorption of materials is essential to identify suitable environmental operating conditions. PTFE/recycled BRS composites were cut into 25.4 mm by 76.2 mm following the ASTM D570 standard. The samples were then immersed in distilled water at 25 °C for 24 h. The percentage of moisture absorption for the composites was calculated according to Equation (1) [18].

$$MA (\%) = \frac{w_f - w_i}{w_i} \times 100 \quad (1)$$

where w_f and w_i are the respective wet and dry weights of the samples.

2.3.3. Density

The density of the PTFE/recycled BRS composites was measured at room temperature using the Archimedes principle. An electronic densitometer (Alfa Mirage Co., Osaka, Japan) was utilised for the measurement. Distilled water was then used as the reference liquid. Hence, the density of the sample was calculated using the following equation [19].

$$\rho_c = \frac{W_{air}}{W_{air} - W_{distilled\ water}} \times \rho_{distilled\ water} \quad (2)$$

where ρ_c is the density of the composite, $\rho_{distilled\ water}$ is the density of distilled water, and w_{air} and $w_{distilled\ water}$ are the weights of the sample in air and distilled water, respectively.

2.3.4. Tensile Strength

The dimensions of PTFE/recycled BRS composites were cut according to the ASTM D638 to determine the tensile strength of the composites [20]. The tensile strength test was conducted at room temperature using a Shimadzu AGS-X 100 kN computerised universal testing machine (UTM, Shimadzu, Kyoto, Japan). The UTM stretched the samples at a 5 mm/min stroke rate with a 10 kN load cell.

2.3.5. Coefficient of Thermal Expansion (CTE)

The CTE of the composites was measured in line with ASTM E228-17 [21]. A push-rod dilatometer, Linseis L75 Platinum (Linseis, Selb, Germany), was used. The measurement was done at room temperature, and the heating rate was set at 10 °C/min.

2.3.6. Complex Permittivity

The complex permittivity of PTFE/recycled BRS composites was characterised using the open-ended coaxial probe (OCP) technique in the 1–12 GHz frequency range [22]. The probe was connected to an Agilent N5227A vector network analyser (Agilent Technologies, Santa Clara, CA, USA), as shown in Figure 1. A one-port reflection calibration technique was used. The one-port calibration technique consists of air, a shorting block and distilled water at 25 °C. After complete calibration, the probe was placed flat on the surface of the samples for characterisation to avoid air gaps between the sample and the open probe that may affect measurement accuracy. A standard (unfilled PTFE) material was first characterised to confirm the accuracy of the calibration. In addition, the dimensions of the composites were 6 cm × 3.6 cm × 0.7 cm.

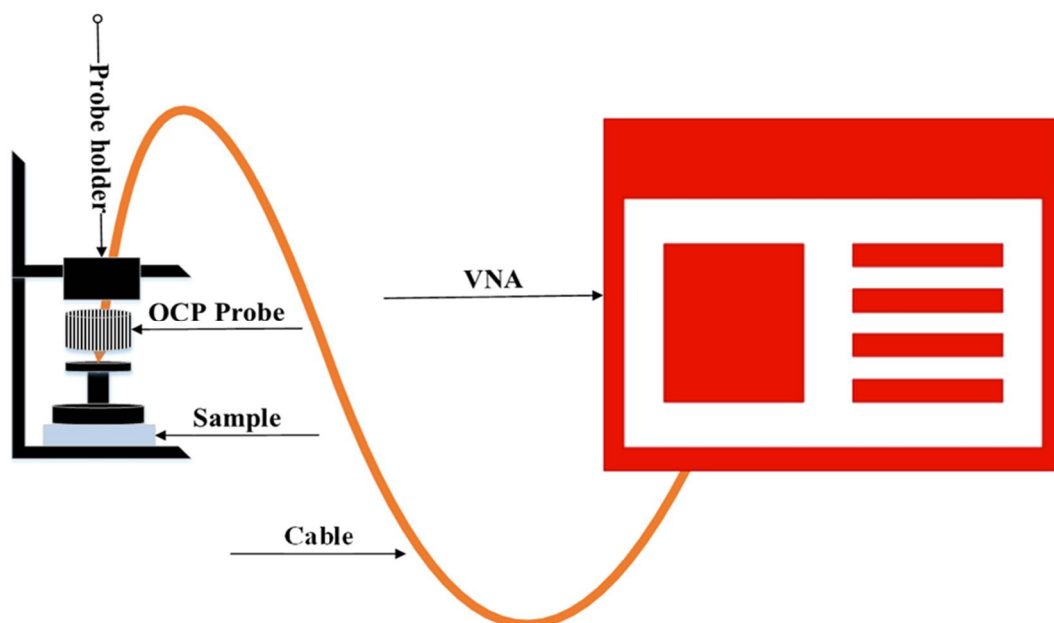


Figure 1. OCP measurement set-up.

The following equation gives the complex permittivity:

$$\varepsilon^* = \varepsilon' - j\varepsilon'' \quad (3)$$

where ε^* is the complex permittivity, ε' is the dielectric constant denoting energy storage, and ε'' is the loss factor, representing energy loss. The loss tangent, being the ratio of loss factor and dielectric constant, is therefore evaluated as follows [23]:

$$\tan\delta = \frac{\varepsilon''}{\varepsilon'} \quad (4)$$

2.3.7. Signal Propagation Speed

A fast signal transmission with minor delay is required to transmit high data. Generally, electromagnetic waves are attenuated when passing through a denser medium. Thus, investigating the influence of filler size on the signal propagation speed is critical to the

design of microwave circuits for efficient data transmission. The signal transmission speed can be calculated using the following equation [24].

$$V_s = \frac{c}{\sqrt{\epsilon' \mu'}} \quad (5)$$

where V_s is the signal transmission speed, c is the speed of light in vacuum, ϵ' is the dielectric constant, and μ' is the permeability of the material.

3. Results and Discussion

3.1. Phase, Morphology and Composition

The X-ray diffraction patterns of 63 μm recycled BRS powder and PTFE/recycled composites are shown in Figure 2. In the 63 μm recycled BRS XRD profile, a broad peak at $2\theta = 15^\circ - 30^\circ$ is observed, confirming the amorphous nature of the recycled BRS glass. This pattern is consistent with the work presented [25], which affirms that no impurities were introduced during the glass powder preparation. The same figure depicts the XRD pattern of PTFE. The diffractogram of the PTFE displays a sharp peak and five low-intensity peaks positioned at $2\theta = 18.05^\circ, 31.53^\circ, 36.60^\circ, 37.13^\circ, 41.18^\circ,$ and 49.07° . These peaks relate to the (100), (110), (200), (107), (108), and (210) planes and are matched with the ICSD index of PTFE (ICSD 00-047-2217) [26,27]. Furthermore, the intensity of the peak located at $2\theta = 18.05^\circ$ can be seen to decrease slightly as different sizes of recycled BRS filler are introduced to the PTFE matrix. In addition, no unwanted peaks in the pattern of the composites indicate that chemical interaction did not occur between the PTFE matrix and recycled BRS particulate.

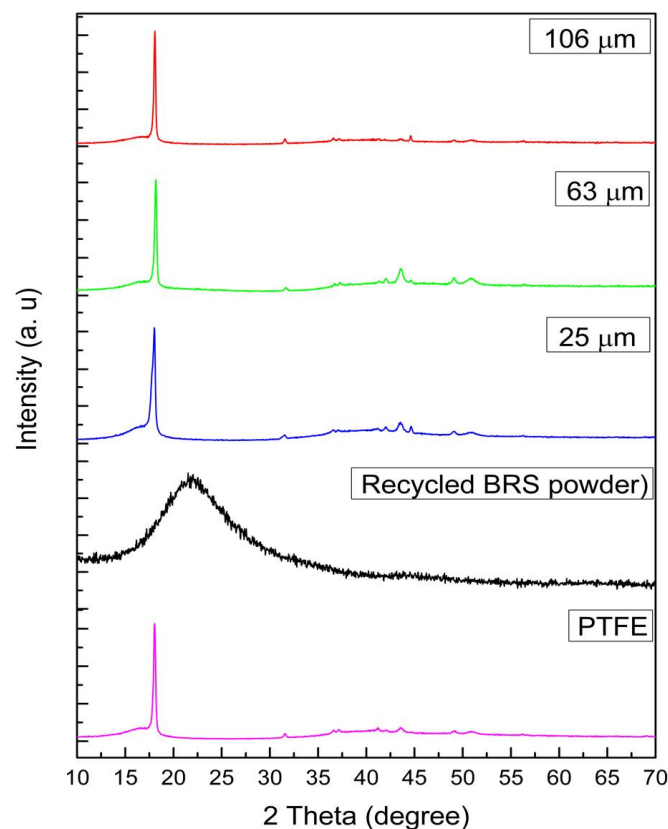


Figure 2. XRD patterns of PTFE, recycled BRS powder and PTFE/recycled BRS composites.

The scanning electron microscope (SEM) images of pure PTFE, 63 μm recycled BRS powder, and PTFE/recycled BRS composites are illustrated in Figure 3. It can be observed that the BRS particles are of arbitrary geometry. The recycled BRS particulates are also more

dispersed in the PTFE matrix at larger filler sizes, indicating a good connection between the PTFE matrix and recycled BRS filler. It is reported that effective dispersion of recycled BRS particulate in the PTFE promotes a homogeneous structure that enhances the properties of the composites [28,29].

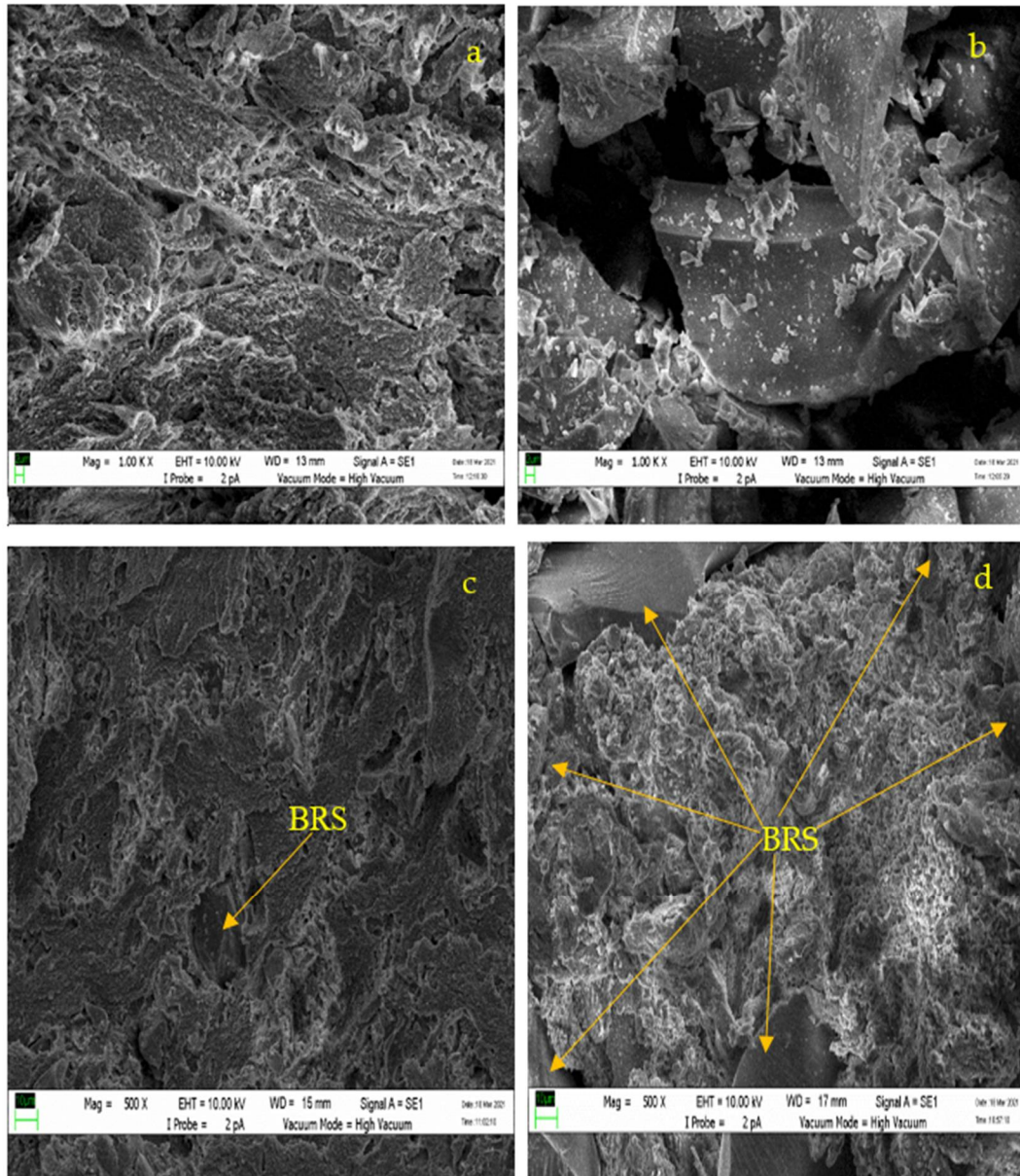


Figure 3. SEM micrographs of (a) PTFE, (b) recycled BRS powder, (c) PTFE/recycled BRS at (at 25 μm BRS) and (d) PTFE/recycled BRS composites at (106 μm BRS).

EDX analysis was conducted to determine the elemental composition of PTFE, 63 μm recycled BRS and PTFE/recycled BRS composites qualitatively. In Figure 4, the spectra show that PTFE comprises mainly C at 0.1 keV and F at 0.5 keV. In addition, the same figure reveals that the 63 μm recycled BRS powder consists of B, O, Na, Al and Si, validating the purity of recycled BRS glass [30]. Further analysis shows that PTFE and recycled BRS glass elements were all present in the PTFE/recycled BRS composites except Na and Al at 25 μm and 106 μm recycled BRS filler loadings. This incidence happens when the concentration level of the respective element falls below the detection limit [31]. Thus, the findings attest to the suitability of the dry powder-processing technique for composite fabrication.

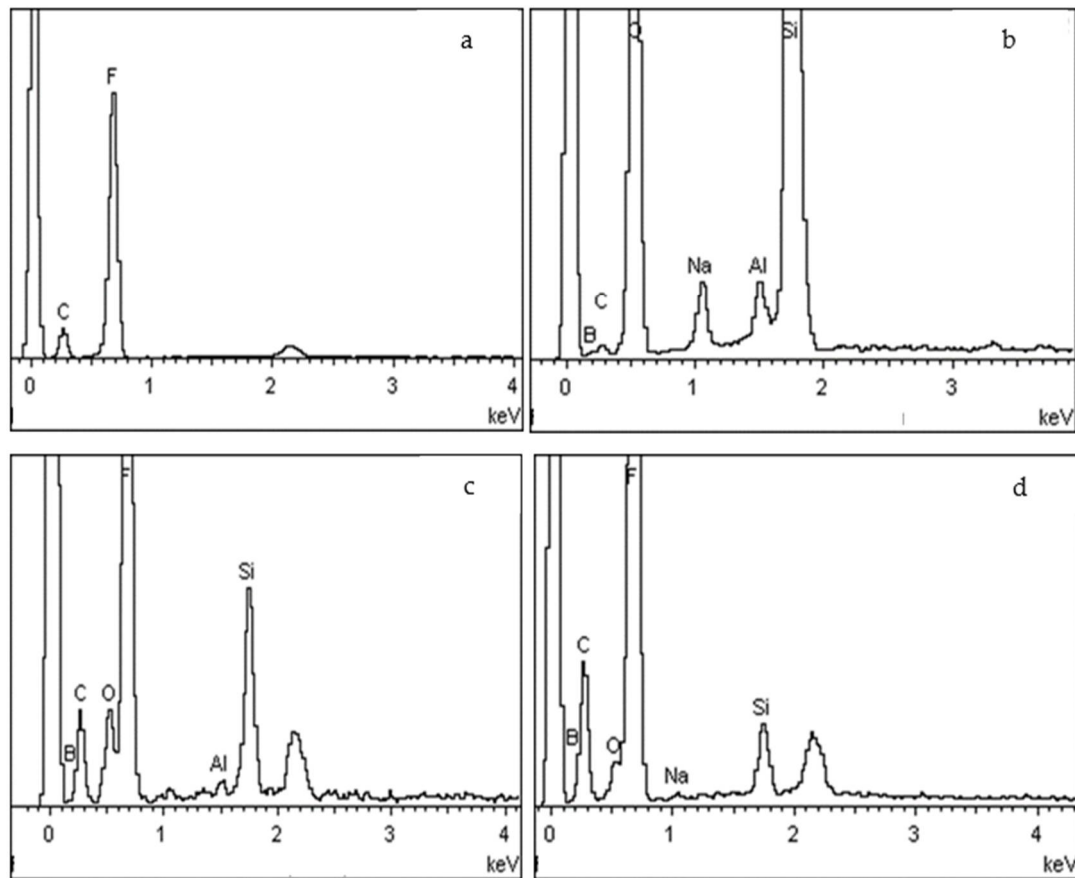


Figure 4. EDX spectra of (a) PTFE, (b) 63 recycled BRS powder, (c) PTFE/recycled BRS at 25 μm BRS and (d) PTFE/recycled BRS at 106 μm BRS.

3.2. Moisture Absorption

Moisture absorption significantly affects composite's dielectric properties because water has a high dielectric constant and loss. It is reported that moisture absorption of $<0.1\%$ is ideal for electronic packaging applications [6,8,32]. Figure 5 shows the variation in the moisture absorption of PTFE/recycled BRS composites. It can be seen that the moisture absorption increases from 0.011% to 0.040% when the recycled BRS filler size is reduced from 106 μm to 25 μm . It is worth noting that the composite records moisture absorption lower than the ideal value recommended. The increase in moisture absorption is attributed to the higher surface area of the smaller-sized recycled BRS particles [8]. Furthermore, the deterioration of moisture absorption is related to the enhanced porosity and density in the composites [33].

3.3. Density

The effect of recycled BRS filler size on the density of the PTFE matrix is shown in Figure 6. The 106 μm , 90 μm , 63 μm , 45 μm , 25 μm , recycled BRS composites had density values of 2.17, 2.18, 2.19, 2.20, and 2.21 g/cm^3 , respectively. Thus, decreasing recycled BRS particle size led to the increase in the density of the composites. A similar result has been reported by Jiang and Yuan [8]. The enhanced density is related to introducing a denser recycled BRS filler than the PTFE matrix [34]. In addition, smaller-sized particles possess more particles per unit volume than larger-sized particles. Therefore, the smaller-sized filler particles occupy less volume, leading to the increased density of the composites. The increase in the density is also due to the higher moisture absorbed by the composites [6,35]. This variation significantly affects the PTFE matrix's CTE, tensile strength and dielectric properties [11].

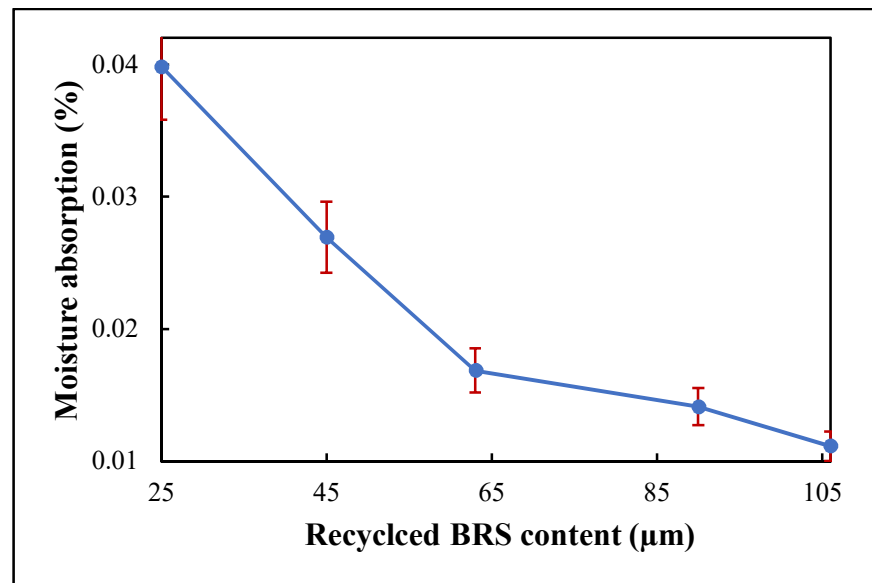


Figure 5. Variation of moisture absorption with filler size.

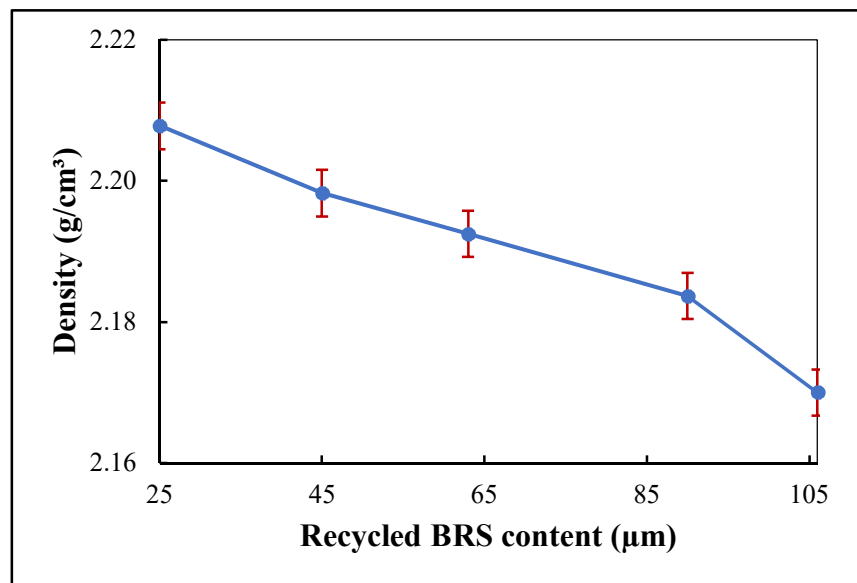


Figure 6. Variation of density with filler size.

3.4. Tensile Strength

The change of tensile strength as a function of recycled BRS particle size is presented in Figure 7. The 106 μm , 90 μm , 63 μm , 45 μm and 25 μm recycled BRS composites had respective tensile strength values of 12.93, 12.93, 12.92, 9.18 and 7.12 MPa. It could be seen that the reduction in particle size corresponded with a decrease in tensile strength consistent with the studies reported [36,37]. Although, the differences in tensile strength at 106 μm , 90 μm and 63 μm BRS sizes are smaller than at 45 μm and 25 μm filler sizes. This reduction in tensile strength is due to poor adhesion between the recycled BRS filler and PTFE matrix [36]. In addition, the smaller-sized particles with a higher surface area tend to absorb more water, which reduced the tensile strength of the PTFE matrix [38,39].

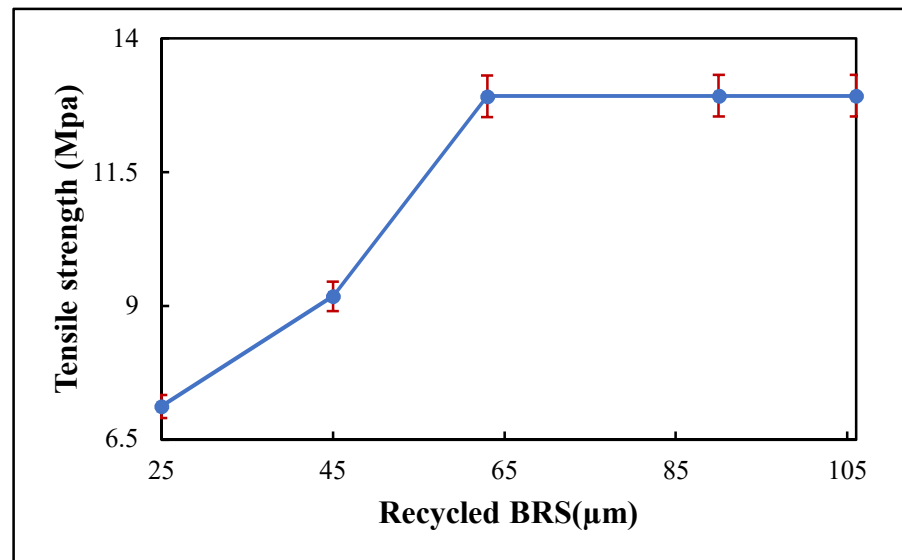


Figure 7. Variation of tensile strength with filler size.

3.5. Coefficient of Thermal Expansion (CTE)

The variation in CTE with recycled BRS particle size is shown in Figure 8. The composites showed a respective CTE of 64.8, 62.33, 60.45, 55.08 and 55.77 ppm/°C at 106 μm, 90 μm, 63 μm, 45 μm and 25 μm filler sizes. It is, therefore, evident that the decrease in filler size matched the drop in the CTE of the composites [8,36]. The variation is first attributed to the mismatch in the CTE of the PTFE matrix (~109 ppm/°C) and the recycled BRS filler (~4 ppm/°C [40,41]). In addition, smaller-sized filler particles have a larger surface area and higher density. Thus, the matrix volume decreases with smaller-sized particles, restricting the matrix expansion, which further reduces the CTE of the composites [12].

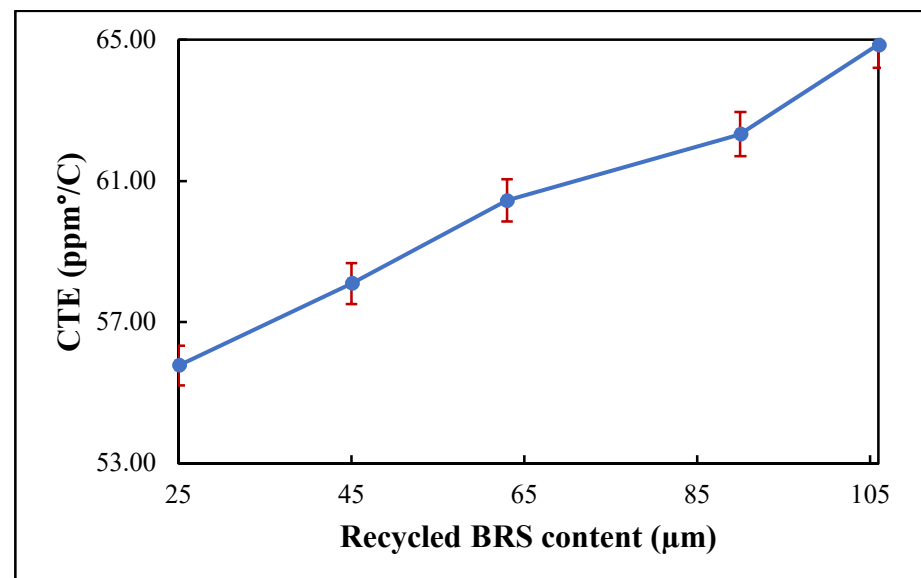


Figure 8. Variation of CTE with filler size.

3.6. Complex Permittivity

The influence of recycled BRS filler size reduction on the dielectric constant and loss factor of PTFE/recycled BRS composites was studied. The variation of ϵ' and ϵ'' in the 1–12 GHz range is presented in Figures 9 and 10, while the calculated $\tan\delta$ is shown in Figure 11. It can be seen that the ϵ' and ϵ'' slightly decreased with the frequency [42–44].

In addition, the ϵ'' had a similar pattern for all composites, which is attributed to the calibration consistent with the loss factor result presented in [45]. The higher values of the ϵ' and ϵ'' at lower frequencies are due to the significant influence of charge relaxation and interfacial polarisation [46]. Generally, as frequency increases, the composite's overall polarisation lags the alternating electric field. Thus, each polarisation process stops contributing, decreasing its dielectric constant and loss factor [47].

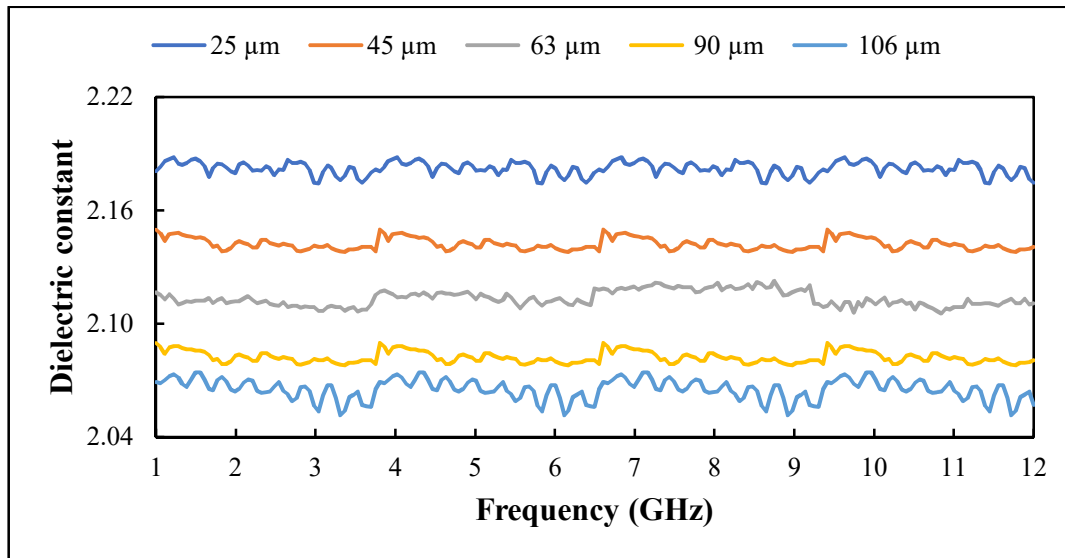


Figure 9. Variation of dielectric constant with filler size.

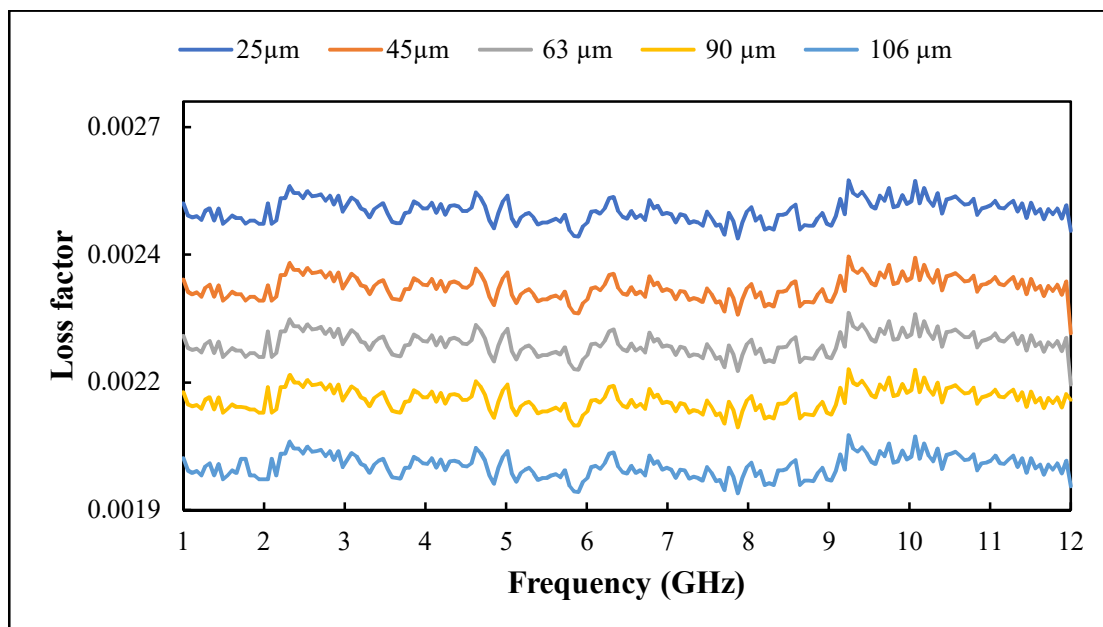


Figure 10. Variation of loss factor with filler size.

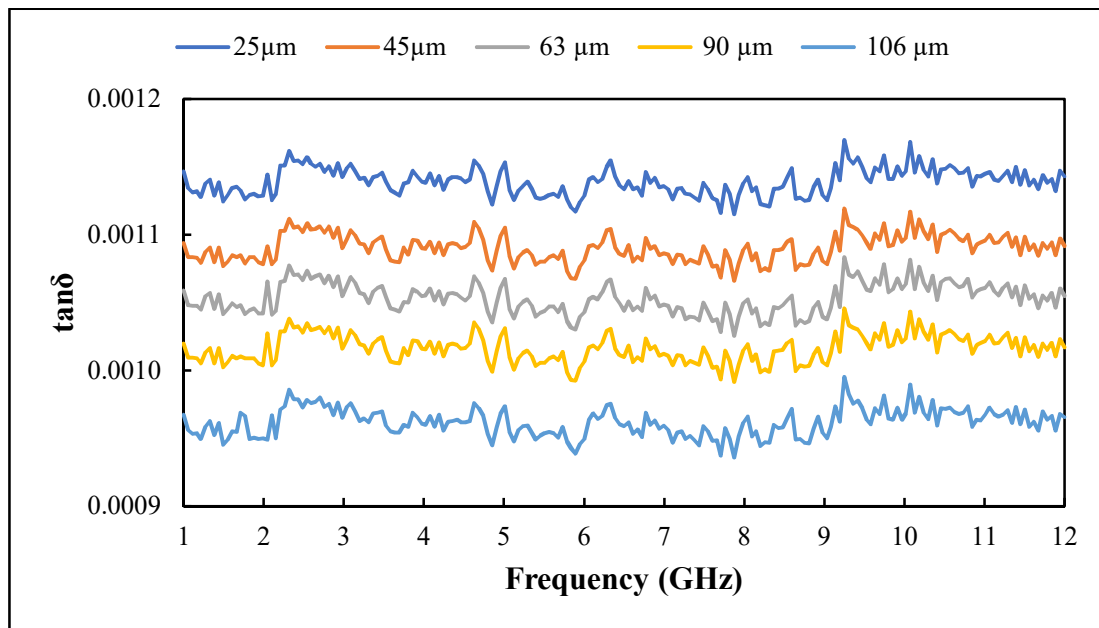


Figure 11. Variation of loss tangent with filler size.

Further analysis showed that the ϵ' and ϵ'' of PTFE/recycled BRS composites increased with the reduction in recycled BRS filler size (Table 2), in agreement with previous work [12,36]. This behaviour is attributed to the higher densification and stronger interfacial polarisation [3]. Composites reinforced with smaller grain-sized particles tend to possess a more significant interfacial area, leading to extra interfacial polarisation, which increases the dielectric properties [12,48]. Moreover, at the same filler content, the number of particulates in the smaller-sized filler is higher than that in the bigger-sized filler. This occurrence leads to a denser composite, which increases the ϵ' and ϵ'' of the composite [12]. At 1 GHz, the values ϵ' and $\tan\delta$ increased from 2.07 and 0.0010 to 2.18 and 0.0011 with a decrement of filler size from 106 μm to 25 μm . Additionally, the values of ϵ' and $\tan\delta$ varied from 2.06 and 0.0010 to 2.17 and 0.0011 at 12 GHz.

Table 2. Mean complex permittivity and loss tangent of PTFE/recycled BRS composites at different filler sizes.

Recycled BRS Size (μm)	ϵ'	ϵ''	$\tan\delta$
25	2.18	0.0026	0.0011
45	2.14	0.0024	0.0011
63	2.11	0.0022	0.0011
90	2.08	0.0021	0.0010
106	2.07	0.0020	0.0010

3.7. Signal Transmission Speed

The variation of signal transmission speed across the PTFE/recycled BRS composites at different recycled BRS sizes and frequencies is depicted in Figure 12. It can be seen that transmission speed decreases with filler size reduction. The higher transmission speed is associated with lower relative permittivity at larger filler sizes. At 1 GHz, PTFE/recycled BRS composites had Vs of 2.032×10^8 m/s, 2.046×10^8 m/s, 2.062×10^8 m/s, 2.075×10^8 m/s and 2.086×10^8 m/s at 25 μm , 45 μm , 63 μm , 90 μm and 106 μm of recycled BRS filler sizes, respectively. The Vs increased to 2.034×10^8 m/s, 2.050×10^8 m/s, 2.065×10^8 m/s, 2.080×10^8 m/s and 2.092×10^8 m/s at 12 GHz for the same filler sizes.

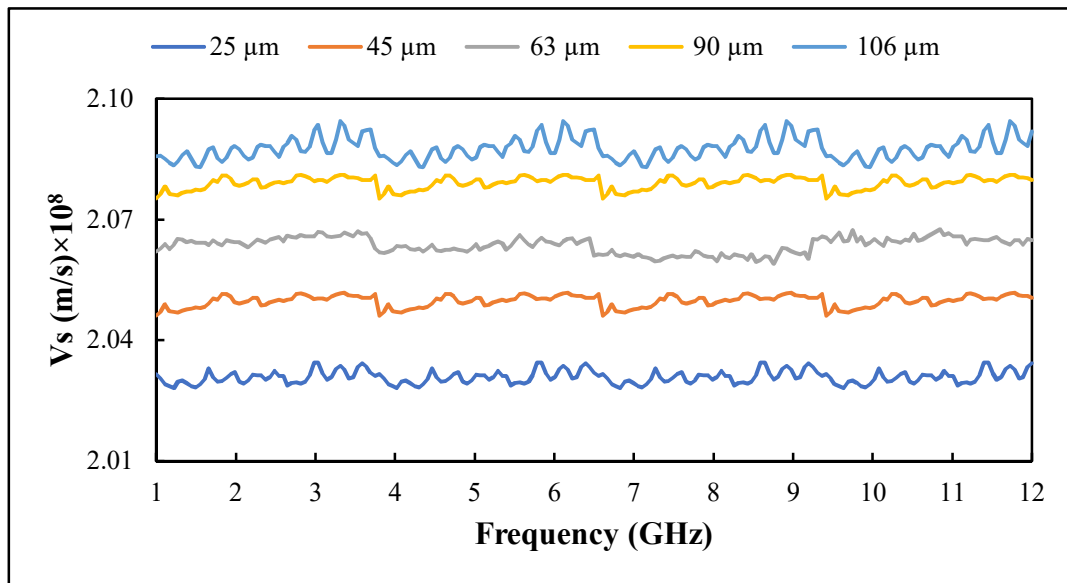


Figure 12. Variation of signal transmission speed with filler size.

The comparison of the PTFE/recycled BRS composite at a filler size of 63 μm with commercial high-frequency laminates is presented in Table 3. The laminates are PTFE-based materials produced by [49,50]. It can be seen that the PTFE/recycled BRS composite shows a lower dielectric constant, loss tangent, moisture absorption and CTE than the laminates. The highest tensile strength is achieved by the TLX-8 laminate, followed by the PTFE/recycled BRS composite. This result proves that recycled BRS glass can reinforce PTFE to produce a low-cost substrate for microwave applications.

Table 3. Comparison between PTFE/recycled BRS composite and commercial high-frequency laminates.

Name	ϵ'	$\tan\delta$	Tensile Strength (MPa)	CTE (ppm/ $^{\circ}\text{C}$)	Moisture Absorption (%)	Reference
	At 10 GHz					
PTFE/recycled BRS composite	2.11 ± 0.05	0.0011 ± 0.00005	12.92 ± 0.005	60.45 ± 0.01	0.02 ± 0.00001	This study
AD250C	2.50	0.0013	6.00	196.00	0.04	[49]
AD255C	2.60	0.0013	8.1	196.00	0.03	[49]
TLX-8	2.55	0.0017	245	215.00	0.02	[50]

4. Conclusions

The PTFE/recycled BRS composites were fabricated through the dry powder processing technique by varying the recycled BRS filler size. XRD profiles of the composites exhibited no unwanted peaks. The scanning electron microscope showed better dispersion of the filler at a larger recycled BRS size. EDX analysis indicated that no foreign element was present in the composites. The complex permittivity of PTFE/recycled BRS composites showed an increasing trend with recycled BRS filler size reduction. The moisture absorption and density of the composites also increased for the same reason. However, the tensile strength, CTE, and signal transmission speed decreased with recycled BRS filler size reduction. At 10 GHz, the 63 μm recycled BRS composite showed suitable dielectric properties ($\epsilon' = 2.11$ and $\tan\delta = 0.0011$), CTE of 60.45 ppm/ $^{\circ}\text{C}$, low moisture absorption of 0.02% and favourable tensile strength of 12.92 MPa, ideal for microwave substrate applications.

Author Contributions: Conceptualization, Z.A. and M.H.M.Z.; formal analysis, I.A.A., Z.A. and A.M.K.; funding acquisition, Z.A.; investigation, I.A.A. and Z.A.; methodology, I.A.A., Z.A. and A.M.K.; resources, Z.A. and M.H.M.Z.; writing—original draft, I.A.A. All authors have read and agreed to the published version of the manuscript.

Funding: This work was supported by the Universiti Putra Malaysia (UPM) and Ministry of Higher Education Malaysia (MOHE) Fundamental Research Grant Scheme: FRGS/1/2015/ICT05/UPM/02/4.

Institutional Review Board Statement: Not applicable.

Informed Consent Statement: Not applicable.

Data Availability Statement: Not applicable.

Acknowledgments: The authors specially thank the Department of Physics (UPM), UPM Holdings & RMC for research management facilities, Sarra Global Sdn Bhd and MOSTI for AG TF0315D031 project, Sunkoo Machine Tech Ltd. for PTFE powder supply, and Ministry of Higher Education (MOHE) Fundamental Research Grant Scheme (FRGS).

Conflicts of Interest: The authors declare no conflict of interest. The funders had no role in the design of the study; in the collection, analyses, or interpretation of data; in the writing of the manuscript, or in the decision to publish the results.

References

1. Manu, K.; Ananthakumar, S.; Sebastian, M. Electrical and thermal properties of low permittivity Sr₂Al₂SiO₇ ceramic filled HDPE composites. *Ceram. Int.* **2013**, *39*, 4945–4951. [[CrossRef](#)]
2. Manu, K.M.; Soni, S.; Murthy, V.R.K.; Sebastian, M.T. Ba(Zn_{1/3}Ta_{2/3})O₃ ceramics reinforced high density polyethylene for microwave applications. *J. Mater. Sci. Mater. Electron.* **2013**, *24*, 2098–2105. [[CrossRef](#)]
3. Xie, C.; Liang, F.; Ma, M.; Chen, X.; Lu, W.; Jia, Y. Microstructure and dielectric properties of PTFE-based composites filled by micron/submicron-blended CCTO. *Crystals* **2017**, *7*, 126. [[CrossRef](#)]
4. Murali, K.P.; Rajesh, S.; Nijesh, K.J.; Ratheesh, R. Effect of particle size on the microwave dielectric properties of alumina-filled PTFE substrates. *Int. J. Appl. Ceram. Technol.* **2010**, *7*, 475–481. [[CrossRef](#)]
5. Rajesh, S.; Murali, K.; Jantunen, H.; Ratheesh, R. The effect of filler on the temperature coefficient of the relative permittivity of PTFE/ceramic composites. *Phys. B Condens. Matter* **2011**, *406*, 4312–4316. [[CrossRef](#)]
6. Varghese, J.; Nair, D.R.; Mohanan, P.; Sebastian, M.T. Dielectric, thermal and mechanical properties of zirconium silicate reinforced high density polyethylene composites for antenna applications. *Phys. Chem. Chem. Phys.* **2015**, *17*, 14943–14950. [[CrossRef](#)]
7. Murali, K.; Rajesh, S.; Prakash, O.; Kulkarni, A.; Ratheesh, R. Preparation and properties of silica filled PTFE flexible laminates for microwave circuit applications. *Compos. Part A Appl. Sci. Manuf.* **2009**, *40*, 1179–1185. [[CrossRef](#)]
8. Jiang, Z.; Yuan, Y. Effects of particle size distribution of silica on properties of PTFE/SiO₂ composites. *Mater. Res. Express* **2018**, *5*, 066306. [[CrossRef](#)]
9. Mazur, K.; Gądek-Moszczak, A.; Liber-Kneć, A.; Kuciel, S. Mechanical behavior and morphological study of polytetrafluoroethylene (PTFE) composites under static and cyclic loading condition. *Materials* **2021**, *14*, 1712. [[CrossRef](#)]
10. Huang, F.; Yuan, Y.; Jiang, Z.; Tang, B.; Zhang, S. Microstructures and properties of glass fiber reinforced PTFE composite substrates with laminated construction. *Mater. Res. Express* **2019**, *6*, 075305. [[CrossRef](#)]
11. Luo, F.; Yuan, Y.; Tang, B.; Yang, J.; Zhang, S. The effects of TiO₂ particle size on the properties of PTFE/TiO₂ composites. *J. Mater. Sci. Chem. Eng.* **2017**, *05*, 53–60. [[CrossRef](#)]
12. Thomas, S.; Kavil, J.; Malayil, A.M. Dielectric properties of PTFE loaded with micro- and nano-Sm₂Si₂O₇ ceramics. *J. Mater. Sci. Mater. Electron.* **2016**, *27*, 9780–9788. [[CrossRef](#)]
13. Francis, L.F. *Powder Processes*; Elsevier: Amsterdam, The Netherlands, 2016; pp. 343–414.
14. Meli, A.D.; Abbas, Z.; Zaid, M.H.M.; Ibrahim, N.A. The effects of SLS on structural and complex permittivity of SLS-HDPE composites. *Adv. Polym. Technol.* **2019**, *2019*, 1–7. [[CrossRef](#)]
15. Ashby, M.F. Materials and the environment. *Phys. Status Solidi A* **1992**, *131*, 625–638. [[CrossRef](#)]
16. Hasanuzzaman, M.; Rafferty, A.; Sajjia, M.; Olabi, A.-G. Properties of glass materials. In *Reference Module in Materials Science and Materials Engineering*; Hashmi, S., Ed.; Elsevier: Amsterdam, The Netherlands, 2016.
17. Kochetov, R.; Tsekmes, I.A.; Morshuis, P.H.F.; Smit, J.J.; Wanner, A.J.; Wiesbrock, F.; Kern, W. Effect of water absorption on dielectric spectrum of nanocomposites. In Proceedings of the 2016 IEEE Electrical Insulation Conference (EIC), Montreal, QC, Canada, 19–22 June 2016; pp. 579–582. [[CrossRef](#)]
18. Zou, C.; Fothergill, J.C.; Rowe, S.W. The effect of water absorption on the dielectric properties of epoxy nanocomposites. *IEEE Trans. Dielectr. Electr. Insul.* **2008**, *15*, 106–117. [[CrossRef](#)]
19. Ismail, N.Q.A.; Saat, N.K.; Zaid, M.H.M. Effect of soda lime silica glass doping on ZnO varistor ceramics: Dry milling method. *J. Asian Ceram. Soc.* **2020**, *8*, 909–914. [[CrossRef](#)]

20. Chaichanawong, J.; Thongchuea, C.; Areerat, S. Effect of moisture on the mechanical properties of glass fiber reinforced polyamide composites. *Adv. Powder Technol.* **2016**, *27*, 898–902. [[CrossRef](#)]
21. Vartak, D.; Ghotekar, Y.; Deshpande, N.; Munjal, B.; Bhatt, P.; Satyanarayana, B.; Vyas, K.; Lal, A. New horizons of space qualification of single-walled carbon nano tubes-carbon fibre reinforced polymer composite. *J. Physics Conf. Ser.* **2021**, *1854*, 012001. [[CrossRef](#)]
22. Mensah, E.E.; Abbas, Z.; Azis, R.S.; Khamis, A.M. Enhancement of complex permittivity and attenuation properties of recycled hematite (α -Fe₂O₃) using nanoparticles prepared via ball milling technique. *Materials* **2019**, *12*, 1696. [[CrossRef](#)]
23. Khamis, A.M.; Abbas, Z.; Ahmad, A.F.; Azis, R.S.; Abdalhadi, D.M.; Mensah, E.E. Experimental and computational study on epoxy resin reinforced with micro-sized OPEFB using rectangular waveguide and finite element method. *IET Microw. Antennas Propag.* **2020**, *14*, 752–758. [[CrossRef](#)]
24. Ratheesh, R.; Sebastian, M. *Polymer-Ceramic Composites for Microwave Applications*; John Wiley & Sons: Hoboken, NJ, USA, 2017; Volume 50, pp. 481–535.
25. Irshidat, M.R.; Al-Saleh, M.H.; Sanad, S. Effect of nanoclay on the expansive potential of cement mortar due to alkali-silica reaction. *ACI Mater. J.* **2015**, *112*. [[CrossRef](#)]
26. Yamaguchi, A.; Kido, H.; Ukita, Y.; Kishihara, M.; Utsumi, Y. Anisotropic pyrochemical microetching of poly(tetrafluoroethylene) initiated by synchrotron radiation-induced scission of molecule bonds. *Appl. Phys. Lett.* **2016**, *108*, 51610. [[CrossRef](#)]
27. Feng, W.; Yin, L.; Han, Y.; Wang, J.; Xiao, K.; Li, J. Tribological and physical properties of PTFE-NBR self-lubricating composites under water lubrication. *Ind. Lubr. Tribol.* **2021**, *73*, 82–87. [[CrossRef](#)]
28. Lago, E.D.; Cagnin, E.; Boaretti, C.; Roso, M.; Lorenzetti, A.; Modesti, M. Influence of different carbon-based fillers on electrical and mechanical properties of a PC/ABS blend. *Polymers* **2019**, *12*, 29. [[CrossRef](#)] [[PubMed](#)]
29. Das, S.; Chattopadhyay, S.; Dhanania, S.; Bhowmick, A.K. Improved dispersion and physico-mechanical properties of rubber/silica composites through new silane grafting. *Polym. Eng. Sci.* **2020**, *60*, 3115–3134. [[CrossRef](#)]
30. Hubert, M.; Faber, A.J. On the structural role of boron in borosilicate glasses. *Phys. Chem. Glas. Eur. J. Glas. Sci. Technol. Part B* **2014**, *55*, 136–158.
31. Nasrazadani, S.; Hassani, S. Modern analytical techniques in failure analysis of aerospace, chemical, and oil and gas industries. In *Handbook of Materials Failure Analysis with Case Studies from the Oil and Gas Industry*; Elsevier: Amsterdam, The Netherlands, 2016; pp. 39–54.
32. Yuan, Y.; Zhang, S.; Zhou, X.; Li, E. MgTiO₃ filled PTFE composites for microwave substrate applications. *Mater. Chem. Phys.* **2013**, *141*, 175–179. [[CrossRef](#)]
33. Wang, H.; Zhou, F.; Guo, J.; Yang, H.; Tong, J.; Zhang, Q. Modified BCZN particles filled PTFE composites with high dielectric constant and low loss for microwave substrate applications. *Ceram. Int.* **2020**, *46*, 7531–7540. [[CrossRef](#)]
34. Hu, Y.; Zhang, Y.; Liu, H.; Zhou, D. Microwave dielectric properties of PTFE/CaTiO₃ polymer ceramic composites. *Ceram. Int.* **2011**, *37*, 1609–1613. [[CrossRef](#)]
35. Murali, K.P.; Rajesh, S.; Jacob, K.S.; Prakash, O.; Kulkarni, A.R.; Ratheesh, R. Preparation and characterization of cordierite filled PTFE laminates for microwave substrate applications. *J. Mater. Sci. Mater. Electron.* **2010**, *21*, 192–198. [[CrossRef](#)]
36. Chen, Y.-C.; Lin, H.-C.; Lee, Y.-D. The effects of filler content and size on the properties of PTFE/SiO₂ composites. *J. Polym. Res.* **2003**, *10*, 247–258. [[CrossRef](#)]
37. Xu, G.; Yu, Y.; Zhang, Y.; Li, T.; Wang, T. Effect of B₄C particle size on the mechanical properties of B₄C reinforced aluminum matrix layered composite. *Sci. Eng. Compos. Mater.* **2019**, *26*, 53–61. [[CrossRef](#)]
38. Mortazavian, S.; Fatemi, A.; Khosrovaneh, A. Effect of water absorption on tensile and fatigue behaviors of two short glass fiber reinforced thermoplastics. *SAE Int. J. Mater. Manuf.* **2015**, *8*, 435–443. [[CrossRef](#)]
39. JA, M.H.; Majid, M.S.A.; Afendi, M.; Marzuki, H.; Hilmi, E.A.; Fahmi, I.; Gibson, A. Effects of water absorption on Napier grass fibre/polyester composites. *Compos. Struct.* **2016**, *144*, 138–146. [[CrossRef](#)]
40. Thomas, D.; Sebastian, M.T. HDPE matrix composites filled with Ca₄La₆(SiO₄)₄(PO₄)₂O₂ for microwave substrate applications. *J. Electron. Packag.* **2014**, *136*, 031002. [[CrossRef](#)]
41. Han, K.; Zhou, J.; Li, Q.; Shen, J.; Qi, Y.; Yao, X.; Chen, W. Effect of filler structure on the dielectric and thermal properties of SiO₂/PTFE composites. *J. Mater. Sci. Mater. Electron.* **2020**, *31*, 9196–9202. [[CrossRef](#)]
42. Elloumi, I.; Koubaa, A.; Kharrat, W.; Bradai, C.; Elloumi, A. Dielectric properties of wood-polymer composites: Effects of frequency, fiber nature, proportion, and chemical composition. *J. Compos. Sci.* **2021**, *5*, 141. [[CrossRef](#)]
43. Rayssi, C.; Kossi, S.E.; Dhahri, J.; Khirouni, K. Frequency and temperature-dependence of dielectric permittivity and electric modulus studies of the solid solution Ca_{0.85}Er_{0.1}Ti_{1-x}Co_{4x}/3O₃ (0 ≤ x ≤ 0.1). *RSC Adv.* **2018**, *8*, 17139–17150. [[CrossRef](#)]
44. Yang, G.; Cui, J.; Ohki, Y.; Wang, D.; Li, Y.; Tao, K. Dielectric and relaxation properties of composites of epoxy resin and hyperbranched-polyester-treated nanosilica. *RSC Adv.* **2018**, *8*, 30669–30677. [[CrossRef](#)]
45. Abdalhadi, D.M.; Abbas, Z.; Ahmad, A.F.; Matori, K.A.; Esa, F. Controlling the properties of OPEFB/PLA polymer composite by using Fe₂O₃ for microwave applications. *Fibers Polym.* **2018**, *19*, 1513–1521. [[CrossRef](#)]
46. Frank Gladson, T.S.; Ramesh, R.; Kavitha, C. Experimental investigation of mechanical, tribological and dielectric properties of alumina nano wire-reinforced PEEK/PTFE composites. *Mater. Res. Express* **2019**, *6*, 115327. [[CrossRef](#)]
47. Khan, M.S.; Osada, M.; Kim, H.-J.; Ebina, Y.; Sugimoto, W.; Sasaki, T. High-temperature dielectric responses in all-nanosheet capacitors. *Jpn. J. Appl. Phys.* **2017**, *56*, 06GH09. [[CrossRef](#)]

-
48. Todd, M.G.; Shi, F.G. Validation of a novel dielectric constant simulation model and the determination of its physical parameters. *Microelectron. J.* **2002**, *33*, 627–632. [[CrossRef](#)]
 49. Advanced Connectivity Solution. AD Series®Laminates 2021:1–4. Available online: <https://rogerscorp.com/advanced-connectivity-solutions/ad-series-laminates> (accessed on 23 January 2021).
 50. Microwave & RF Laminates Products. TLX High Volume Fiberglass Reinforced Microwave Substrate 2020. Available online: <https://www.agc-multimaterial.com/page/microwave--rf-laminates-66.html> (accessed on 5 July 2021).